ADVANCED OPTICAL MATERIALS
www.advopticalmat.de

Multimodal Visualization of Bioorthogonal Systems by Off–On Luminescence and Enhanced Magnetic Resonance Imaging

Chen Xie, Yue Wu, Ho-Fai Chau, Tao Zhang, Carlos Tinlong Wong, Yik-Hoi Yeung, Pak-Lun Lam, Jean-Claude G. Bünzli, Loïc J. Charbonnière,* Ga-Lai Law,* and Ka-Leung Wong**

Bioorthogonal chemistry is a rising field investigating chemical reactions in physiological environments with high specificity. However, only very few examples concern the real-time monitoring of bioorthogonal reactions by luminescence or magnetic relaxivity. To fill this gap, herein, the Eu(III)-based complex is reported as a small-molecule optical imaging agent which shows off–on luminescence and provides quantitative analysis for the progress of the bioorthogonal reaction. The characteristic signal is achieved through efficient energy harvesting and transferring to the Eu(III) from the expansion of the conjugated system of the antenna. Moreover, the gadolinium(III) counterpart significantly enhances relaxivity in magnetic resonance imaging (MRI) after the bioorthogonal reaction since the rotational correlation time is shortened with increased molecular sizes and weights.

1. Introduction

It was monumental when Bertozzi et al. introduced the term "Bioorthogonal Chemistry" in 2003.[1] Those scientists proposed that researchers would be able to perform reactions in complex biological environments rather than under harsh conditions in organic solvents. There have been many impressive applications of bioorthogonal chemistry in recent years, including molecular imaging, protein lipidation, and in vivo diagnosis.[2–4] Although it is common to probe and monitor cellular processes by bioorthogonal reactions, the real-time monitoring of the bioorthogonal reaction progress is also important and usually achieved by organic fluorophores.[5]

Lanthanide luminescence shows its great potential for biomedical imaging and analysis.[6] Emission from lanthanides mostly features much longer lifetimes (microsecond-scale) than those from common organic luminophores (nanosecond-scale), so the time-resolved detection is available that largely improves the signal-to-noise ratio. Although lanthanide trivalent ions show impressive luminescence properties, their absorption coefficient is quite low. Therefore, a suitable antenna, which can harvest excitation energy and transfer it efficiently to the lanthanide-excited states, is required.[7]

There are only a few reports concerning the application of luminescent lanthanide complexes in bioorthogonal chemistry,

C. Xie, Y. Wu, H.-F. Chau, Y.-H. Yeung, P.-L. Lam, K.-L. Wong
Department of Chemistry
Hong Kong Baptist University
224 Waterloo Rd, Kowloon Tong, Kowloon, Hong Kong SAR, P. R. China
E-mail: klwong@hkbu.edu.hk

C. Xie, L. J. Charbonnière
Equipe de synthèse pour l'analyse (SynPA)
Institut Pluridisciplinaire Hubert Curien (IPHC)
Département des sciences analytiques (DSA) - UMR 7178
CNRS/Université de Strasbourg
ECPM
Bâtiment R1N0, 25, rue Becquerel, 67087 Strasbourg Cedex 2, France
E-mail: l.charbonn@unistra.fr

The ORCID identification number(s) for the author(s) of this article can be found under https://doi.org/10.1002/adom.202203057.

DOI: 10.1002/adom.202203057

T. Zhang
MOE Key Laboratory of Laser Life Science & Institute of Laser Life Science
Guangdong Provincial Key Laboratory of Laser Life Science, and College of Biophotonics
South China Normal University
Guangzhou 510631, P. R. China
E-mail: zt@scnu.edu.cn

C. T. Wong, G.-L. Law
Department of Applied Biology and Chemical Technology
State Key Laboratory of Chemical Biology and Drug Discovery
The Hong Kong Polytechnic University
Hong Kong, P. R. China
E-mail: ga-lai.law@polyu.edu.hk

J.-C. G. Bünzli
Institut des Sciences et Ingénierie Chimiques
École Polytechnique Fédérale de Lausanne (EPFL)
1015, Lausanne, Switzerland

and few of them feature off–on properties. In 2016, O'Malley et al. prepared Tb(III) complexes that can conjugate to biomolecules through a click reaction between an alkyne group and an azide group.[8] The successful conjugation would result in a significant Tb(III) emission enhancement. However, the usage of Cu(I) catalyst inevitably causes cytotoxicity from the resulting Cu(I) salts. Another example was reported by Zheng and his co-workers in 2020.[9] A biocompatible Tb(III) complex underwent ligation with cell surface glycans that resulted in a large increase in luminescence. It is because the cycloaddition reaction changed the electronic structures of the linked quencher, and the energy transfer from the antenna to Tb(III) was promoted. Jin et al. recently synthesized and characterized a series of lanthanide-based bioorthogonal probes for NIR cell imaging.[10] Noteworthily, most reported examples always feature emitters working independently that generate light before the bioorthogonal reactions. It possibly brings wrong interpretations on the targeting sites and reaction progress while an off–on probe can avoid these problems.

Click reaction is ideal to be applied in bioorthogonal chemistry because it is usually considered to be highly specific and requires no heating.[11] For example, Cu(I)-catalyzed azide–alkyne cycloaddition (CuAAC) is commonly used for nucleic acid labeling.[12] However, "copper-free" click chemistry is much more attractive to bioorthogonal chemists from the view of biocompatibility. There are several strategies to process click reactions without copper catalysts, including the strain-promoted azide–alkyne cycloadditions (SPAAC).[13] The cyclooctynes with high strain, which are eight-membered ring cyclooctynes in most cases, tend to react with azide spontaneously without the aid of metal catalysts. Although the second-order rate constant of the early reported cyclooctynes was only 0.0012 M^{-1} s^{-1}, much lower than those of CuAAC (k_2 = 10–200 M^{-1} s^{-1}),[14] the cyclooctynes with higher reactivity, like dibenzocyclooctyne (DBCO; also called aza-dibenzocyclooctyne) were developed as representatives. At a physiological temperature and pH range, DBCO does not easily react with endogenous amines/hydroxyls that means they are relatively inert to most biomolecules, while they are reacting with azide groups at much higher rates than with thiol groups.[15] This reagent allows copper-free click reactions in living organisms and prefers cycloadditions with azide groups. It features the fusion of dibenzo systems that improves the reactivity of its cycloalkynes.[16] Besides, a nitrogen atom on its strained ring also decreases the molecular hydrophobicity and eases the probe conjugation, which facilitates specific reactions with azides.[17] The second-order reaction rate constant for DBCO groups with azide groups is around 1 M^{-1} s^{-1}, nearly one thousand times higher than some early reported cyclooctynes.[18]

We herein reported lanthanide-based complexes, **LnBT**, featuring a Ln(III)-coordinated DO3A-azidopyridine conjugate. It can specifically perform metal-free SPAAC reactions with DBCO derivatives, where DBCOs are readily available and capable of subsequent conjugation with other biomolecules through their carboxylic groups. The second-order reaction rate constant of the cycloaddition between LnBT and DBCO derivatives was determined as 0.39 ± 0.007 M^{-1} min^{-1} by nuclear magnetic resonance (NMR) techniques with lanthanum(III) counterpart LaBT. Prior to SPAAC reactions, the Eu complex, **EuBT**, emits negligible light with an excitation wavelength from 200 to 400 nm. After the cycloaddition with DBCOs, the formed triazolyl links the pyridine ring of the lanthanide complex and two benzene rings of DBCO together to give an expanded conjugated system. The expanded conjugated system featured a lower excited energy level and therefore enabled the efficient energy transfer to the Eu(III) center to generate strong visible light (Figure S1, Supporting Information), where the emission intensity was proportional to the extent of this bioorthogonal reaction (**Figure 1**a). This reaction and the antenna-expanding strategy show broad application and fill the gap of monitoring bioorthogonal chemistry by off–on luminescence. Furthermore, the Gd(III) counterpart **GdBT** also showed enhancement in magnetic relaxivity over cycloaddition. We presented a series of kinetic studies by applying our complexes to **DBCO-COOH** or **DBCO-Man** (DBCO-mannosamine conjugate). The progressive signaling could realize the visualization of the bioorthogonal reaction process by instant luminescence changes, and also exhibits the potential of our modal serving as a promising agent in targeted diagnosis.

2. Results and Discussion

The LnBT was obtained by a concise synthetic route (Figure 1b). The commercially available starting material (4-bromopyridin-2-yl)methanol (1) was converted into (4-azidopyridin-2-yl)methanol (2) by heating with sodium azide in the water-DMF mixed solvent. 2 was then methanesulfonated and installed onto DO3A core by S_N2 reaction to give 3. The desired LnBT complexes were obtained after deprotection of *tert*-butyl of 3, then coordinated with corresponding lanthanide salt.

Although the kinetics of most DBCO derivatives have been fully investigated in previous studies, here the azido group in LnBT is linked to an aromatic system rather than to an alkyl chain in most other cases. Therefore, the reaction rate constants between DBCOs and LnBT should be revisited. We performed a series of automated ^{1}H NMR spectroscopic measurements by mixing the DBCO-COOH and LaBT in d^4-methanol. The diamagnetic lanthanum counterpart was used for avoiding signal interference found in most other paramagnetic lanthanides. Although DBCO-Man and aqueous solutions were studied for other studies in our work, they were not ideal in NMR studies requiring much higher concentrations and bringing solubility problems. The samples were mixed in an NMR tube and monitored by the NMR signals for up to 780 min (**Figure 2**a). Before the reaction started (0 min), there was a doublet peak located at around 8.5 ppm attributed to the proton on the *ortho*-position of the nitrogen atom of pyridinyl group (Figure 2a, red spot). With the reaction processing, the doublet peak shifted downfield and turned to be a pair of broad peaks, which represent the two configurational isomers of postclick products. After 600 min, the original peak at around 8.5 ppm was completely shifted to around 8.7 ppm, which means the LaBT was fully consumed. Considering the peak integral at $t = 0$ corresponding to the initial concentration of LaBT, the instantaneous concentrations can be calculated at different time points and plotted (Figure 2b). The curve exhibits a nonlinear decay, which suggests the reaction was not of zero order.

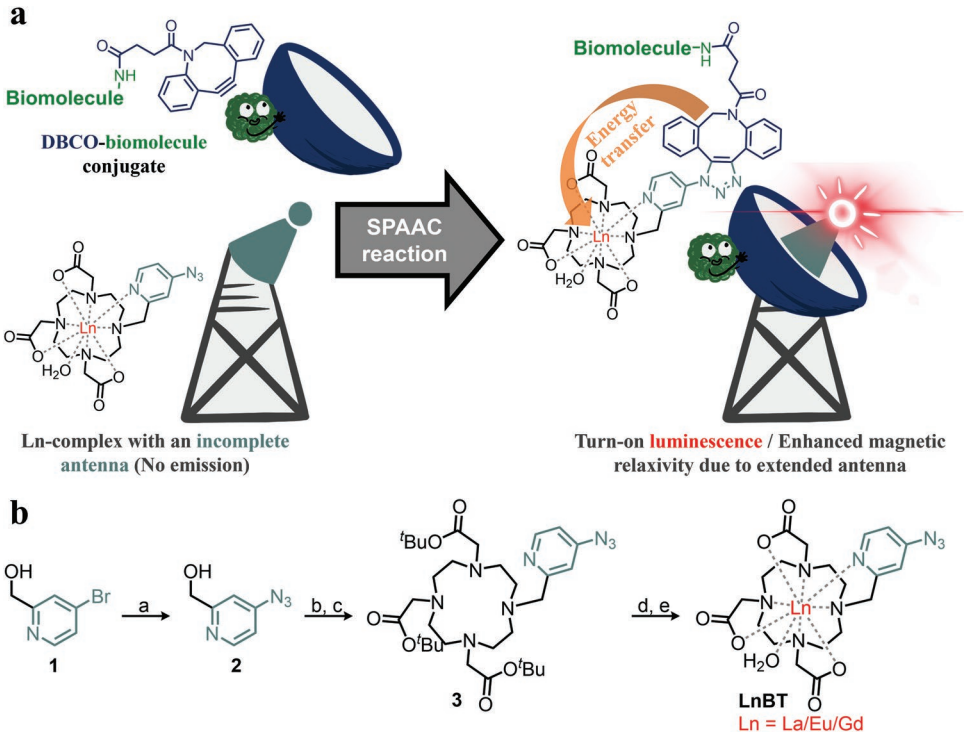

Figure 1. a) The illustration of the off–on luminescence generation process. The SPAAC reaction expands the antenna and makes it suitable to transfer excitation energy to the Eu(III) center. Also, for Gd(III) counterpart, the SPAAC reaction enlarges the molecular weight that results in the enhancement of magnetic relaxivity. b) Synthetic route of desired compounds. Reagent and conditions: a. NaN_3, DMF/H_2O, v/v, 20/1, 90 °C, 14 d; b. MsCl, DIPEA, DCM, 0 °C →r.t., 30 min; c. ^{t}Bu-DO3A, K_2CO_3, MeCN, 50 °C, 24 h; d. TFA/DCM, v/v, 1/1, 16 h, r.t.; e. $LnCl_3{\cdot}nH_2O$, H_2O/MeOH, pH 7–8, 12 h, r.t.

Considering a standard second-order reaction, A + B → Product, we have

$$-\frac{dx}{dt} = -k[\mathrm{A}][\mathrm{B}] = -k\left([\mathrm{A}]_0 - x\right)\left([\mathrm{B}]_0 - x\right) \tag{1}$$

Integrating the equation from 0 to t, we have

$$\frac{1}{[\mathrm{B}]_0 - [\mathrm{A}]_0} \ln \frac{[\mathrm{B}][\mathrm{A}]_0}{[\mathrm{A}][\mathrm{B}]_0} = kt \tag{2}$$

where x is the concentration of each species reacted at time t, so (dx/dt) represents the instantaneous reaction rate; [A] and [B] are the concentrations of LaBT complex and DBCO-COOH, respectively. We can obtain the instant [A] by comparing the NMR peak integrals and calculate the concentration of B by

$$[\mathrm{B}] = [\mathrm{B}]_0 - [\mathrm{A}] \tag{3}$$

By plotting the logarithmic expression of the concentrations versus time (t), we obtained the reaction rate constant k from its slope (Figure 2c) in the dynamic range (0–270 min). The reaction rate constant k was determined from the slope as 3.92×10^{-4} mM^{-1} min^{-1} (0.39 M^{-1} min^{-1}). This value is smaller than those in the literature for SPAAC between azide and DBCO, because most previous works studied alkyl azides, whereas we focused on azidopyridine where the electrons were stabilized on the conjugated π-bond system and less reactive.

To further confirm that the SPAAC reaction between DBCO derivative and LnBT can preserve high specificity under an aqueous condition, the HPLC and mass spectrometry were applied (**Figure 3**) on 0.8 mM GdBT and 1.2 mM DBCO-Man (DBCO-biomolecule conjugate) in the HEPES buffer. DBCO-Man can be synthesized from DBCO-COOH by a single-step reaction with mannosamine (Figure S2, Supporting Information), a metabolic precursor on the cell surface.[19] The retention time of GdBT and DBCO-Man is 14.7 and 39.3 min, respectively, under given HPLC conditions (Table S1, Supporting Information). The GdBT was mostly consumed after the reaction mixture was placed at room temperature for 24 h, while excess DBCO-Man remained. Two newly formed peaks, in very close retention time, were found at 26.0 and 27.1 min, respectively. The structures of two peaks were characterized by mass spectrometry and confirmed as two configurational isomers of expected postclick products.

Lanthanide luminescence is the key indicator for the off–on property and the evaluation of the bioorthogonal progress in our case. One of the important advantages of our EuBT complex is its off–on luminescent properties. Emission spectra were obtained from a reacting solution of EuBT and DBCO-Man at different time points (**Figure 4**a). With 320-nm light irradiation, the EuBT alone has no light emission before the conjugation, but after the addition of DBCO derivatives and then the successful SPAAC reaction, the Eu(III) center will be effectively sensitized and produce long-lived, characteristic visible emission. The emission intensity is enhanced with the progression of the reaction and the formation of conjugated

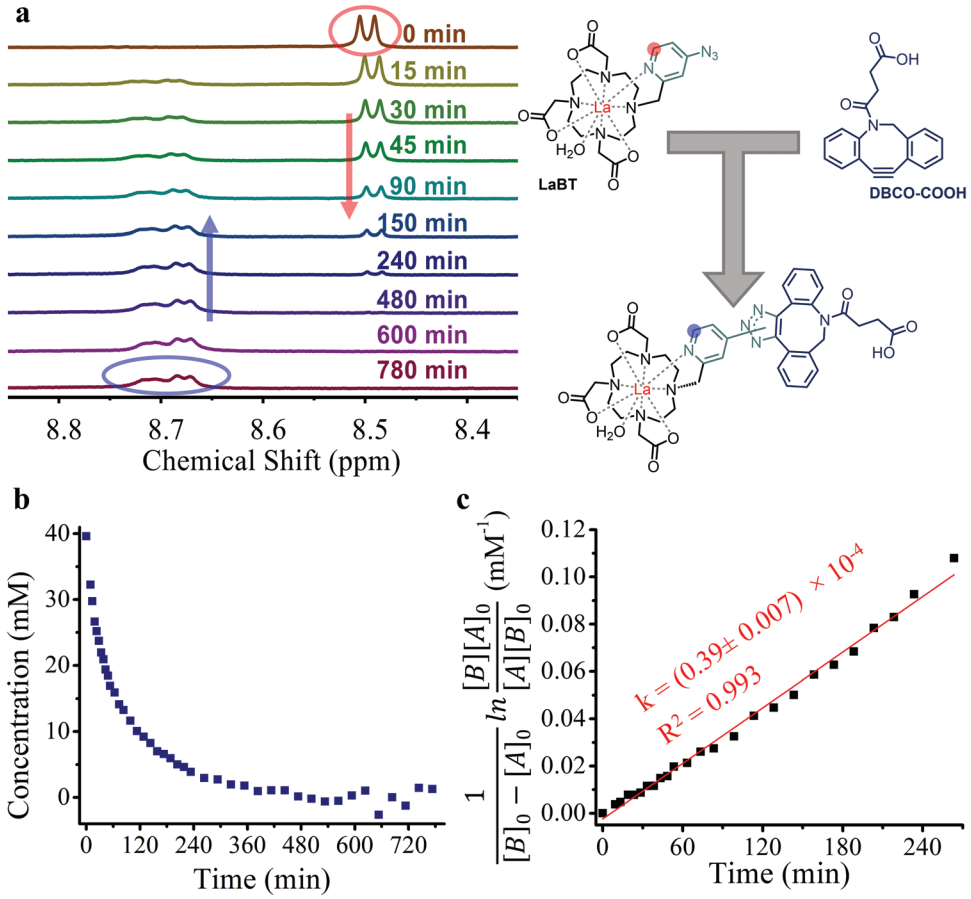

Figure 2. a) Overlapping ^{1}H NMR spectra of LaBT and DBCO-COOH mixing solutions in d^4-methanol at different time points. b) The plot of the calculated concentrations of LaBT (by the NMR peak integrals at 8.5 ppm) versus reaction time. c) Logarithmic plot of the reaction of LaBT with DBCO-COOH in d^4-methanol.

products. Strong Eu(III) emission was observed after 5 min of the reaction. After 240 min, EuBT had mostly been reacted and the emission intensity was 9.2 times stronger compared with the signal at t = 2 min by monitoring 699 nm emission. Emission intensities at 615 and 699 nm were plotted and well fitted with single-exponential functions (Figure 4b). The excitation spectra were obtained by monitoring the 615 nm Eu(III) hypersensitive emission peak. We had no observable excitation peak for EuBT. However, for the bioorthogonal product from EuBT and DBCO-Man, it was found to be sensitized by light ranging from 230 to 350 nm (Figure S4a, Supporting Information). The EuBT had no observable emission peaks when excited either by 260 or 320 nm (Figure S4b,c, Supporting Information). On contrary, the bioorthogonal product showed emission peaks at 578, 588, 615, 652, and 699 nm assigned to Eu(III) transitions $^5D_0 \rightarrow {}^7F_J$ (J = 0, 1, 2, 3, 4), respectively (Figure 4a). In a majority of luminescence spectra for Eu(III) materials, the $^5D_0 \rightarrow {}^7F_2$ transitions feature the most intense emission peaks. However, in our case, the $^5D_0 \rightarrow {}^7F_4$ transition dominated while $^5D_0 \rightarrow {}^7F_2$ was much weaker. This phenomenon was also found in other Eu(III)-DO3A complexes.[20,21] Binnemans et al.[22] claimed that Eu(III)-complexes with D_{4d} symmetry have intense $^5D_0 \rightarrow {}^7F_4$ transitions because of the absence of a center of symmetry but the $^5D_0 \rightarrow {}^7F_2$ transition is forbidden. As for Ln(III)-*tetra*-substituted cyclen chelates, they usually adopt either a monocapped twisted square antiprismatic geometry or a monocapped square antiprismatic (SAP) geometry where SAP geometry has a perfect D_{4d} symmetry. Even though our complex does not feature a pure SAP geometry, the partial similarity has already resulted in an intense $^5D_0 \rightarrow {}^7F_4$ emission peak.

We further investigated the change of magnetic relaxivity of the analog, GdBT, that coordinates with gadolinium. Gd^{3+} is commonly used for magnetic resonance imaging because this paramagnetic element can enhance nuclear relaxation rates.[23] We performed in vitro MR imaging for different samples before the bioorthogonal reaction or at the different extents of reactions (**Figure 5**a), and the obvious brightening effects could be found after 4 h. The r_1 relaxivity was calculated (Table S2, Supporting Information), and that of GdBT was determined as 3.2 mM^{-1} s^{-1} prior to the bioorthogonal reaction. By mixing with DBCO-Man in an aqueous solution, the r_1 relaxivity was increasing as the progress of a bioorthogonal reaction. After 4 h reaction, the r_1 relaxivity of the reaction mixture approached 4.4 $mM^{-1}s^{-1}$, which is similar to Gd-DOTA, a commonly used MRI agent (r_1 = 4.5 $mM^{-1}s^{-1}$ in our measurement). Noteworthily, ManNAc (*N*-acetyl-*D*-mannosamine monohydrate), featuring the same sugar unit as Man,

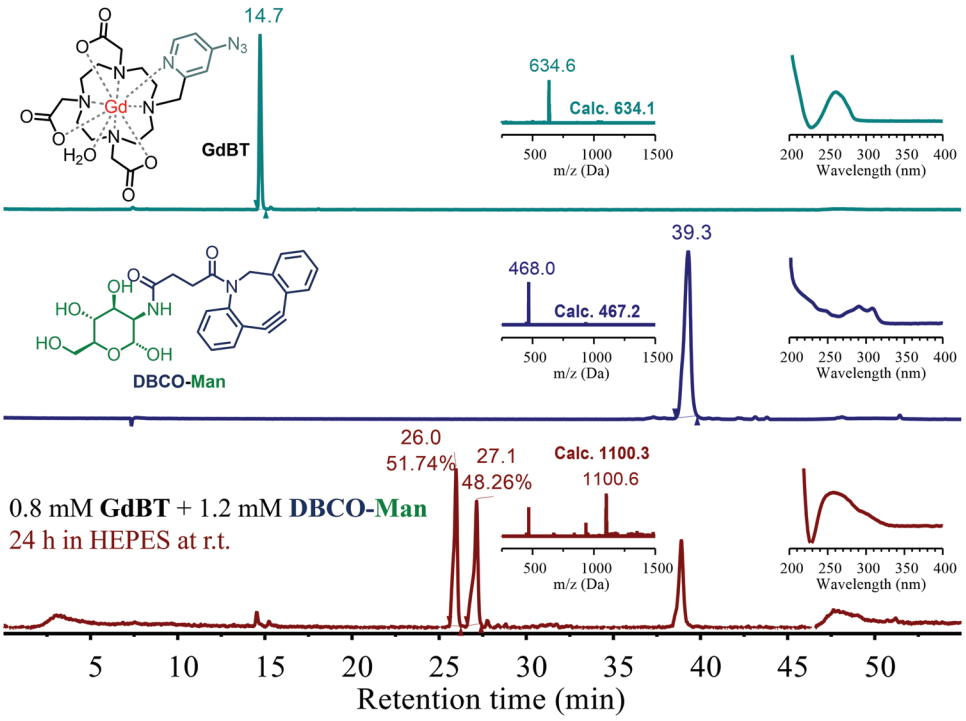

Figure 3. HPLC chromatograph of GdBT (top), DBCO-Man (middle), and postclick reaction mixture (bottom) with online UV–vis spectra of the corresponding peaks and ESI-MS spectra of two starting materials and reacting mixture.

has been reported with a half-life of ≈2.4 h by oral administration, and it reached the maximal plasma concentration after 4 h,[24] which is adequate for the bioorthogonal reaction revealing enhanced magnetic resonance contrast. After 24 h reaction, the r_1 relaxivity of the reaction mixture is up to 5.5 mM^{-1} s^{-1}, which showed around 72% enhancement over bioorthogonal reaction (Figure 5b,c). The signal enhancement resulted from the increase of rotational correlation time due to the enlargement of molecular weight over reaction progress. Through bioorthogonal reactions, our Gd(III)-analog revealed alternative imaging capacity in addition to light signals, and specific MRI/dual-modal imaging could be developed.

3. Conclusion

In this work, to address the limitations in reaction-progress monitoring for bioorthogonal chemistry, we successfully applied expanding-antenna strategies on a series of lanthanide-based complexes by specific bioorthogonal reactions. A nonemissive complex, EuBT, can generate highly differentiated light signals while being involved in bioorthogonal reactions. The relatively long-lived signal features both off–on properties and quantification of the products. Its gadolinium counterpart, GdBT, also showed MRI signal enhancement over bioorthogonal-reaction progress. Hence, we report a novel bioorthogonal model that could facilitate solving emerging problems in biomedical imaging.

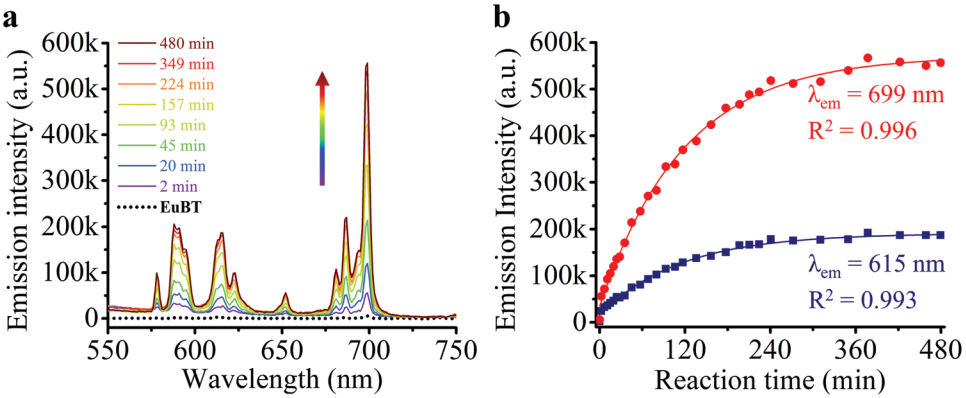

Figure 4. a) Emission spectra of the solution for an ongoing bioorthogonal reaction between EuBT (2 mM) and DBCO-Man (oversaturated) at different time points. The reaction and the measurement were both performed at room temperature in HPEPS, λ_{ex} = 320 nm. b) The changes in the intensity versus time of emission peaks at 615 and 699 nm. Both curves are fitted with single exponential functions.

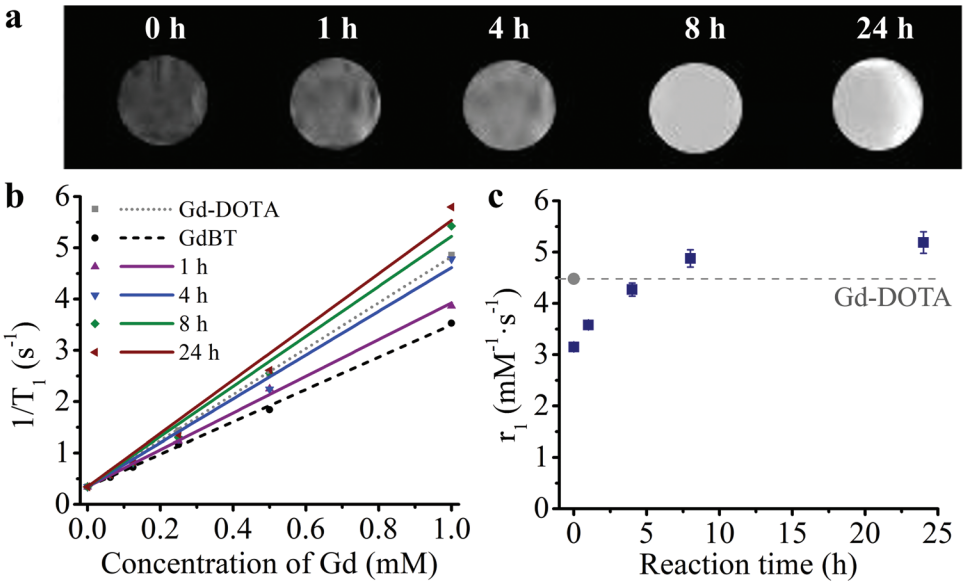

Figure 5. The change of relaxivity of GdBT reacting with DBCO-Man, measured in water, at 25 °C, 1.0 T. a) The reaction was visualized by in vitro MR imaging. b) The plot for linear fitting of the $1/T_1$ and the concentration of Gd containing substances. c) The change of r_1 relaxivity over time.

Supporting Information

Supporting Information is available from the Wiley Online Library or from the author.

Received: December 20, 2022
Revised: January 18, 2023
Published online: March 8, 2023

Acknowledgements

C.X. and Y.W. contributed equally to this work. G.-L.L. gratefully acknowledges The Hong Kong Polytechnic University ((a) University Research Facility in Chemical and Environmental Analysis (UCEA); (b) University Research Facility in Life Sciences (ULS)) and the Hong Kong Research (grant Nos. 15300919, 15301120, and 153021/18P). K.-L.W. gratefully acknowledges the financial assistance from the Hong Kong Research Grants Council (grant No. 12300021), Dr. Mok Man Hung Endowed Professorship in Chemistry, HKBU–Durham Lanthanide Joint Research Center – Lanthanide Tools for Systems Medicine (grant No. SDF19-1011-P02), and the Centre for Medical Engineering of Molecular and Biological Probes (grant No. AoE/M-401/20).

Conflict of Interest

The authors declare no conflict of interest.

Data Availability Statement

The data that supports the findings of this study are available in the supplementary material of this article.

Keywords

bioorthogonal chemistry, lanthanides, luminescence, magnetic resonance imaging

[1] H. C. Hang, C. Yu, D. L. Kato, C. R. Bertozzi, *Proc. Natl. Acad. Sci. USA* **2003**, *100*, 14846.
[2] H. C. Hang, J. P. Wilson, G. Charron, *Acc. Chem. Res.* **2011**, *44*, 699.
[3] N. K. Devaraj, G. M. Thurber, E. J. Keliher, B. Marinelli, R. Weissleder, *Proc. Natl. Acad. Sci. USA* **2012**, *109*, 4762.
[4] P. Dong, X. Wang, J. Zheng, X. Zhang, Y. Li, W. Wu, L. Li, *Curr. Med. Chem.* **2020**, *27*, 3924.
[5] P. Shieh, C. R. Bertozzi, *Org. Biomol. Chem.* **2014**, *12*, 9307.
[6] J.-C. G. Bünzli, *Chem. Rev.* **2010**, *110*, 2729.
[7] J. C. Bünzli, C. Piguet, *Chem. Soc. Rev.* **2005**, *34*, 1048.
[8] W. I. O'Malley, E. H. Abdelkader, M. L. Aulsebrook, R. Rubbiani, C. T. Loh, M. R. Grace, L. Spiccia, G. Gasser, G. Otting, K. L. Tuck, B. Graham, *Inorg. Chem.* **2016**, *55*, 1674.
[9] J. Zheng, Q. Zhan, L. Jiang, D. Xing, T. Zhang, K.-L. Wong, *Inorg. Chem. Front.* **2020**, *7*, 4062.
[10] G.-Q. Jin, D.-e. Sun, X. Xia, Z.-F. Jiang, B. Cheng, Y. Ning, F. Wang, Y. Zhao, X. Chen, J.-L. Zhang, *Angew. Chem., Int. Ed.* **2022**, *61*, e202208707.
[11] H. C. Kolb, M. G. Finn, K. B. Sharpless, *Angew. Chem. Int. Ed.* **2001**, *40*, 2004.
[12] H. El-Sagheer, T. Brown, *Chem. Soc. Rev.* **2010**, *39*, 1388.
[13] N. J. Agard, J. N. Prescher, C. R. Bertozzi, *J. Am. Chem. Soc.* **2004**, *126*, 15046.
[14] K. Wang, A. Sachdeva, D. J. Cox, N. M. Wilf, K. Lang, S. Wallace, R. A. Mehl, J. W. Chin, *Nat. Chem.* **2014**, *6*, 393.
[15] P. D. Zhang, A. A. Vinogradov, Z. P. Gates, B. L. Pentelute, *Angew. Chem. Int. Ed. Engl.* **2018**, *57*, 6459.
[16] X. Ning, J. Guo, M. A. Wolfert, G. J. Boons, *Angew. Chem. Int. Ed. Engl.* **2008**, *47*, 2253.
[17] E. M. Sletten, C. R. Bertozzi, *Org. Lett.* **2008**, *10*, 3097.
[18] P. Ramil, Q. Lin, *Chem. Commun.* **2013**, *49*, 11007.

[19] S. G. Sampathkumar, A. V. Li, K. J. Yarema, *Nat. Protoc.* **2006**, *1*, 2377.
[20] H. Li, C. Xie, R. Lan, S. Zha, C. F. Chan, W. Y. Wong, K. L. Ho, B. D. Chan, Y. Luo, J. X. Zhang, G. L. Law, W. C. S. Tai, J. G. Bunzli, K. .L. Wong, *J. Med. Chem.* **2017**, *60*, 8923.
[21] S. R. Kiraev, E. Mathieu, F. Siemens, D. Kovacs, E. Demeyere, K. E. Borbas, *Molecules* **2020**, *25*, 5282.
[22] K. Binnemans, *Coord. Chem. Rev.* **2015**, *295*, 1.
[23] H. Li, T. J. Meade, *J. Am. Chem. Soc.* **2019**, *141*, 17025.
[24] X. Xu, A. Q. Wang, L. L. Latham, F. Celeste, C. Ciccone, M. C. Malicdan, B. Goldspiel, P. Terse, J. Cradock, N. Yang, S. Yorke, J. C. McKew, W. A. Gahl, M. Huizing, N. Carrillo, *Mol. Genet. Metab.* **2017**, *122*, 126.